to record the responses from individual layer 2/3 pyramidal cells together with their presynaptic partners in different cortical layers. Presynaptic cells within layers 2/3 and 4 (and, to some extent, layer 5) are tuned similarly for motion direction and orientation, forming layer-specific functional modules. The preferred direction and orientation of different layer modules can be aligned, resulting in presynaptic networks that are "feature-locked," or can be shifted relative to each other, giving rise to "feature-variant" networks (Fig. 4C).

The existence of feature-locked and feature-variant networks may explain why some studies found more variability than others in the tuning of dendritic input sites of layer 2/3 pyramidal cells (*6*–*8*) and may suggest that variability is likely due to inputs from deeper cortical layers. The combination of distinct layer modules in feature-variant networks is consistent with previous studies in brain slices showing cross-talk between different subnetworks in layer 2/3 and layer 5 (*18*, *19*). In the visual cortex, the strength of connections among neurons correlates with similarity in visual responses (*20*), raising the possibility that feature-locked networks have a higher density of strong connections compared with feature-variant networks. Also, whether different subtypes of cortical interneurons (*21*, *22*) are differentially represented in feature-locked and feature-variant networks remains an open question. Finally, it will be interesting to test whether postsynaptic cells in feature-locked and feature-variant networks exhibit different population coupling strengths (*23*).

What could be the role of feature-variant presynaptic networks? One possibility is that feature-variant networks are plastic. Top-down modulation or learning (*24*) could force the preferred direction and orientation of layer modules to align, resulting in a transition from a feature-variant to a feature-locked network. This recruitment of relevant circuits could allow more robust feature representations of behaviorally important stimuli. Another possibility is that variant layer modules enhance responses of the postsynaptic cell during object motion. Approaching and receding objects, for example, have edges moving in different directions. Some of these edges may stimulate inputs from deeper layers, which are not strong enough to drive responses of the postsynaptic cell alone but could boost responses of the postsynaptic cell to an edge moving in its preferred direction. Indeed, responses to combinations of orientations have been demonstrated in primate V2 (*25*).

### REFERENCES AND NOTES


1. D. H. Hubel, T. N. Wiesel, *J. Physiol.* **148**, 574–591 (1959).
2. U. C. Dräger, *J. Comp. Neurol.* **160**, 269–290 (1975).
3. T. Hafting, M. Fyhn, S. Molden, M.-B. Moser, E. I. Moser, *Nature* **436**, 801–806 (2005).
4. W. A. Freiwald, D. Y. Tsao, M. S. Livingstone, *Nat. Neurosci.* **12**, 1187–1196 (2009).
5. H. Ko *et al.*, *Nature* **473**, 87–91 (2011).
6. S. L. Smith, I. T. Smith, T. Branco, M. Häusser, *Nature* **503**, 115–120 (2013).
7. H. Jia, N. L. Rochefort, X. Chen, A. Konnerth, *Nature* **464**, 1307–1312 (2010).
8. T.-W. Chen *et al.*, *Nature* **499**, 295–300 (2013).
9. J. H. Marshel, T. Mori, K. J. Nielsen, E. M. Callaway, *Neuron* **67**, 562–574 (2010).
10. I. R. Wickersham *et al.*, *Neuron* **53**, 639–647 (2007).
11. E. A. Rancz *et al.*, *Nat. Neurosci.* **14**, 527–532 (2011).
12. M. Vélez-Fort *et al.*, *Neuron* **83**, 1431–1443 (2014).
13. S. Schuett, T. Bonhoeffer, M. Hübener, *J. Neurosci.* **22**, 6549–6559 (2002).
14. Y.-J. Liu *et al.*, *Curr. Biol.* **23**, 1746–1755 (2013).
15. K. D. Harris, G. M. G. Shepherd, *Nat. Neurosci.* **18**, 170–181 (2015).
16. M. Mazurek, M. Kager, S. D. Van Hooser, *Front. Neural Circuits* **8**, 92 (2014).
17. G. Katona *et al.*, *Nat. Methods* **9**, 201–208 (2012).
18. B. M. Kampa, J. J. Letzkus, G. J. Stuart, *Nat. Neurosci.* **9**, 1472–1473 (2006).
19. Y. Yoshimura, J. L. M. Dantzker, E. M. Callaway, *Nature* **433**, 868–873 (2005).
20. L. Cossell *et al.*, *Nature* **518**, 399–403 (2015).
21. C. A. Runyan *et al.*, *Neuron* **67**, 847–857 (2010).
22. A. M. Kerlin, M. L. Andermann, V. K. Berezovskii, R. C. Reid, *Neuron* **67**, 858–871 (2010).
23. M. Okun *et al.*, *Nature* **521**, 511–515 (2015).
24. J. P. Gavornik, M. F. Bear, *Nat. Neurosci.* **17**, 732–737 (2014).
25. A. Anzai, X. Peng, D. C. Van Essen, *Nat. Neurosci.* **10**, 1313–1321 (2007).
26. K. Kitamura, B. Judkewitz, M. Kano, W. Denk, M. Häusser, *Nat. Methods* **5**, 61–67 (2008).
27. B. Judkewitz, M. Rizzi, K. Kitamura, M. Häusser, *Nat. Protoc.* **4**, 862–869 (2009).


### ACKNOWLEDGMENTS

We thank R. da Silveira for helpful discussions about possible functional roles for feature-locked and -variant networks. We thank S. Oakeley and A. Drinnenberg for commenting on the manuscript and members of the Facility for Advanced Imaging and Microscopy at the Friedrich Miescher Institute (FMI) for assistance with anatomical data acquisition and image processing. Original data are curated and stored in the server of FMI. All materials described in this paper, with the exception of the rabies virus, can be obtained for noncommercial purposes after signing a material transfer agreement (MTA) with FMI. The rabies virus can be obtained for noncommercial purposes after signing an MTA with the Ludwig-Maximilians-University Munich. The plasmids can be obtained from Addgene (addgene.org). We acknowledge the following grants: Human Frontier Science Program Postdoctoral Fellowship (LT000173/2013) to S.T.; Japan Society for the Promotion of Science Postdoctoral Fellowship for Research Abroad to K.Y.; European Molecular Biology Organization Postdoctoral Fellowship to D.H.; Swiss National Science Foundation grant to G.K.; Swiss-Hungarian, Hungarian-French, Central-Hungarian Region, Research and Technological Innovation Fund and European Union 3x3D Imaging grants to B. Rózsa; German Research Foundation Neuronal Circuits grant (SFB 870) to K.-K.C. and A.G.; Gebert-Ruf Foundation, Swiss National Science Foundation, European Research Council, National Centres of Competence in Research Molecular Systems Engineering, Sinergia, Swiss-Hungarian, and European Union 3X3D Imaging grants to B. Roska. Author contributions: In vivo electroporation and virus tracing techniques were optimized by A.W. Experiments were designed by A.W., S.T., and B. Roska. Experiments were performed by A.W. and S.T. Image data analysis was performed by A.W. Immunohistochemistry was performed by A.W. and S.T. Morphological data analysis was performed by S.T. Stimulation software was written by Z.R. Two-photon microscopes were developed by B. Rózsa and optimized by G.S. and D.H. Rabies virus was developed by A.G. and K.-K.C. Plasmids were made by K.Y. The intrinsic imaging was performed by A.W., M.L., and G.K. The paper was written by A.W., S.T., and B. Roska.

### SUPPLEMENTARY MATERIALS

www.sciencemag.org/content/349/6243/70/suppl/DC1
Materials and Methods
Figs. S1 to S15
References (*28*–*35*)

20 March 2015; accepted 29 May 2015
10.1126/science.aab1687

BRAIN STRUCTURE

# Cortical folding scales universally with surface area and thickness, not number of neurons

**Bruno Mota[1] and Suzana Herculano-Houzel[2,3]***

**Larger brains tend to have more folded cortices, but what makes the cortex fold has remained unknown. We show that the degree of cortical folding scales uniformly across lissencephalic and gyrencephalic species, across individuals, and within individual cortices as a function of the product of cortical surface area and the square root of cortical thickness. This relation is derived from the minimization of the effective free energy associated with cortical shape according to a simple physical model, based on known mechanisms of axonal elongation. This model also explains the scaling of the folding index of crumpled paper balls. We discuss the implications of this finding for the evolutionary and developmental origin of folding, including the newfound continuum between lissencephaly and gyrencephaly, and for pathologies such as human lissencephaly.**

The expansion of the cerebral cortex, the most obvious feature of mammalian brain evolution, is generally accompanied by increasing degrees of folding of the cortical surface into sulci and gyri (*1*). Cortical folding has been considered a means of allowing numbers of neurons in the cerebral cortex to expand beyond what would be possible in a lissencephalic cortex, presumably as the cortical sheet expands laterally with a constant number of neurons beneath the surface (*2*, *3*). Although some models have shown cortical convolutions

[1]Instituto de Física, Universidade Federal do Rio de Janeiro, Rio de Janeiro, Brazil. [2]Instituto de Ciências Biomédicas, Universidade Federal do Rio de Janeiro, Rio de Janeiro, Brazil. [3]Instituto Nacional de Neurociência Translacional, INCT/MCT, São Paulo, Brazil.
***Corresponding author. E-mail: suzanahh@gmail.com**

Downloaded from www.sciencemag.org on July 2, 2015

to form as a result of cortical growth (*4*, *5*), the mechanisms that drive gyrification remain to be determined, and the field still lacks a mechanistic and predictive, quantitative explanation for how the degree of cortical folding scales across species. Moreover, recent systematic analyses of cortical folding have made clear that gyrification actually scales differently across mammalian orders, across clades within an order, and across individuals as a function of increasing brain volume (*6*–*9*). These apparent discrepancies have led to the view that different mechanisms must regulate cortical folding at the evolutionary, species-specific, and ontogenetic levels (*7*).

We undertook a systematic analysis of the variation in cortical folding across a large sample of mammalian species in search of a universal, unifying relationship between cortical folding and morphological properties of the cerebral cortex. We examined two data sets: our own, which includes numbers of cortical neurons and cortical surface areas (*10*–*21*), and another consisting of published data on cortical surface area, thickness, brain volume, and folding index, but not numbers of cortical neurons (*1*, *22*–*24*) (table S1).

In the combined data set, there is a general correlation between total brain mass and the degree of cortical folding, and the two data sets overlap in their distribution (Fig. 1A, compare black and colored data points). However, the power function that relates the folding index of gyrencephalic species to brain mass has a fairly low $r^2$ and a 95% confidence interval that excludes many species (Fig. 1A). Striking and well-known outliers in this relationship are cetaceans (as a whole) and the manatee, but the capybara, the greater kudu, and humans also lie outside of the confidence interval (Fig. 1A). This indicates that cortical folding is not a homogeneous function of brain mass.

Although all cortical hemispheres with fewer than 30 million neurons are lissencephalic in our data set, and the correlation between folding index and number of neurons is significant across gyrencephalic species (Spearman correlation, $\rho$ = 0.7741, $P < 0.0001$), the degree of gyrification is much larger in artiodactyls than in primates for similar numbers of cortical neurons (Fig. 1B). Additionally, the elephant cortex is about twice as folded as the human cortex, although the former has only about one-third the number of neurons found in the latter (Fig. 1B, "e" and "h"). The cortical surface area across species expands sublinearly with the number of cortical neurons in primates and supralinearly in other species (Fig. 1C). As a consequence, the average number of neurons per $mm^2$ of cortical surface is highly variable across species, ranging in our data set from 10,752 in the African elephant (*15*) to 138,606 in the squirrel monkey (*20*). Cortical expansion and folding are therefore neither a direct consequence of increasing numbers of neurons nor a requirement for increasing numbers of neurons in the cortex.

In comparison to the poor fit between folding index and total brain mass (Fig. 1A), a better fit is found for total surface area of the cerebral cortex in the two data sets (Fig. 1D). In this case, there is better overlap across afrotherians, glires, primates, and artiodactyls, although cetaceans, the manatee, and humans are still major outliers. Interestingly, all species with a cortical surface area below 400 $mm^2$ are lissencephalic in the two data sets. Similarly, all species with average cortical thickness below 1.2 mm are lissencephalic, but the folding index does not vary as a significant power function of cortical thickness across gyrencephalic species (Fig. 1E).

The folding index shows a sharp inflection between smooth and gyrated cortices, so it is unlikely that a universal model in terms of this variable alone could be derived. Because the folding index is the ratio of total surface area $A_G$ to exposed surface area $A_E$, we next examined directly how $A_E$ scales with $A_G$ (Fig. 1F). In the combined data sets, for the species with small $A_G$ (<400 $mm^2$) there is no folding, such that $A_E$ equals $A_G$ (Fig. 1F, green

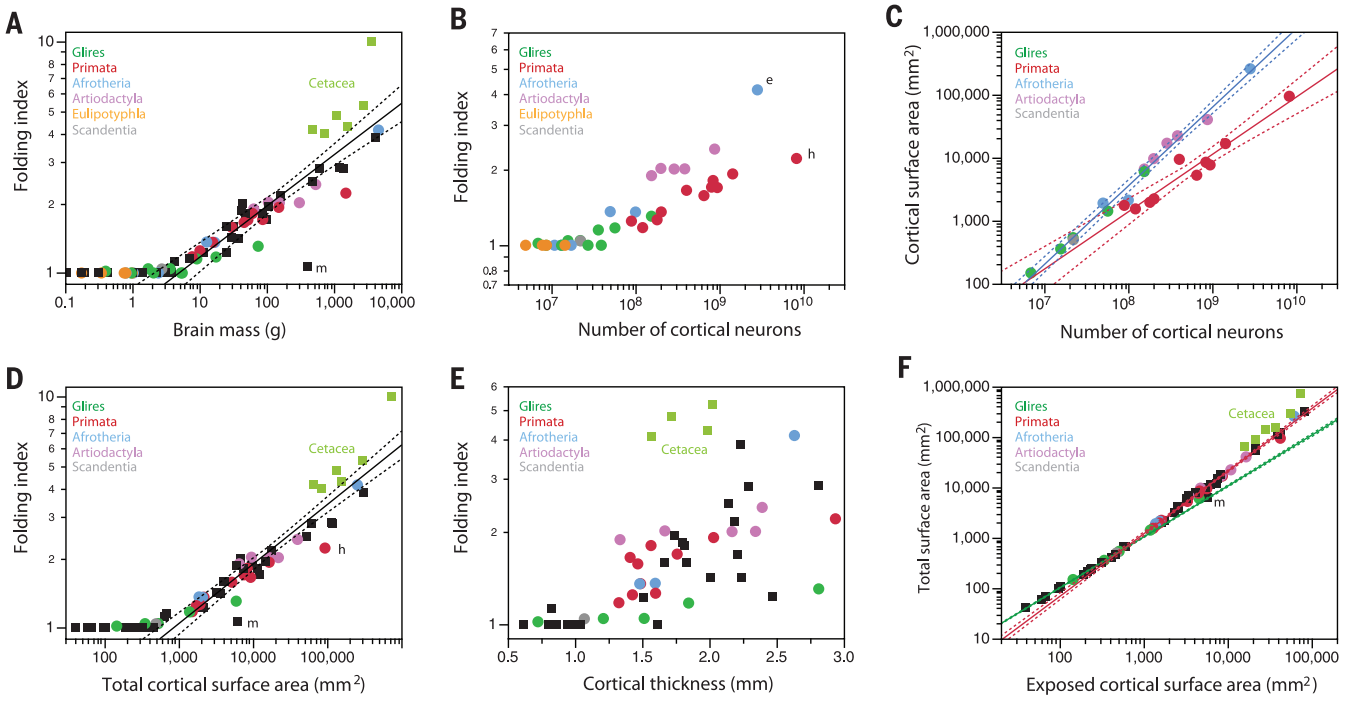


**Fig. 1. Scaling of cortical folding index and total cortical surface area.** Data points in black are taken from the literature; points in colors are from our own data set, except for cetaceans. (**A** to **E**) Folding index scales across all gyrencephalic species in the combined data sets as power functions of (A) brain mass, with exponent 0.221 ± 0.018 ($r^2$ = 0.751, $P < 0.0001$); (B) number of cortical neurons, with exponent 0.168 ± 0.032 ($r^2$ = 0.573, $P < 0.0001$; not plotted); (D) total cortical area, with exponent 0.257 ± 0.014 ($r^2$ = 0.872, $P < 0.0001$); and (E) average cortical thickness, with a nonsignificant exponent ($r^2$ = 0.054, $P$ = 0.1430; not plotted). (C) Total cortical surface area of the cerebral cortex scales across primate species with an exponent of 0.911 ± 0.083 ($r^2$ = 0.938, $P < 0.0001$) and across nonprimate species with an exponent of 1.248 ± 0.037 ($r^2$ = 0.989, $P < 0.0001$). (**F**) Total cortical surface area varies across lissencephalic species as a linear function of the exposed surface area, but as a power function with an exponent of 1.242 ± 0.018 across noncetacean gyrencephalic species ($r^2$ = 0.992, $P < 0.0001$). Dashed lines are 95% confidence intervals for the fitted functions.

line). This linear relationship extends to the manatee cerebral cortex, even though its $A_G$ is much larger than 1000 mm$^2$. In contrast, for all noncetacean gyrencephalic species, $A_G$ increases with $A_E^{1.242\pm0.018}$ ($r^2$ = 0.992, $P$ < 0.0001), significantly above linearity (Fig. 1F, red line), meaning that as total surface area increases, it becomes increasingly folded. Cetaceans fall above the 95% confidence interval of the function, which indicates that these cortices are more folded than similarly sized cortices in noncetaceans.

The finding that $A_G$ scales as a power law of $A_E$ means that gyrification is a property of a cortical surface that is self-similar down to a fundamental scale (the limit area between lissencephaly and gyrencephaly). This strongly suggests the existence of a single universal mechanism responsible for cortical folding (the alternative being some improbable multiscale fine-tuning) that over a range of scales generates self-similar, or fractal, surfaces.

Fractals can be characterized by the power-law scaling between intrinsic and extrinsic measures of an object's size, such as $A_G$ and $A_E$. In this case, the fractal dimension $d$ of the cortical surface is twice the value of the exponent relating $A_G$ to $A_E$ (given that $A_E$ in turn scales with the square of the linear dimension of the cortex). Given that $A_G$ scales with $A_E^{1.242\pm0.018}$ across noncetacean gyrencephalic brains, then $d$ = 2.484 ± 0.036. This value is remarkably close to the fractal dimension 2.5 of crumpled sheets of paper (*25*), which are fractal-like self-avoiding surfaces thin enough to fold under external compression while maintaining structural integrity.

Empirically, we conceive the fractal folding (or lack thereof) of the cortical surface as a consequence of the minimization of the effective free energy of a self-avoiding surface of average thickness $T$ that bounds a volume composed of fibers connecting distal regions of said surface. Our model incorporates the known mechanics and organization of elongating axonal fibers (*26*, *27*), as described in the supplementary materials. It predicts that from a purely physical perspective, $A_G$, $A_E$, and $T$ are related by the power law $T^{1/2}A_G = kA_E^{5/4}$. (The exponent 5/4 is the only value for which the constant $k$ is adimensional.)

We first tested whether our model based on the minimization of the effective free energy of a self-avoiding surface could explain the well-known fractal folding of a self-avoiding surface: paper. We examined how the exposed surface area of crumpled paper balls, $A_E$, scales with increasing total surface area, $A_T$, and thickness, $T$, of office paper (in this case, under forces applied externally by the experimenter's hands). As shown in Fig. 2A, $A_T \approx A_E^{1.234\pm0.033}$ for crumpled single sheets, a value similar to that for gyrencephalic cortices. Increasing $T$ (by stacking sheets before crumpling) displaces the curves to the right (Fig. 2A) but leaves their slope largely unaltered, resulting in similar-looking but less folded paper balls (Fig. 2B). However, the product $T^{1/2}A_T$ varies proportionately to $A_E^{1.105\pm0.022}$ as a single, universal power function across all paper balls of different surface areas and thicknesses (Fig. 2C), as predicted by our model. This conformity indicates that the coarse-grained folding of a sheet of paper subjected to external compression depends simply on a combination of its surface area and thickness.

We next examined whether our model predicts the folding of the mammalian cerebral cortex by plotting the product $T^{1/2}A_G$ as a function of $A_E$ for the combined data sets. This yielded a power function with an exponent of 1.329 ± 0.014, with a very high $r^2$ of 0.996 for the noncetacean gyrencephalic species in the combined data sets (Fig. 3A, red line). Note that this function, although calculated for gyrencephalic species, overlaps with lissencephalic species. Including lissencephalic species (but still excluding cetaceans) actually improved the fit, with $r^2$ = 0.998, and yielded an exponent of 1.305 ± 0.010, which is close to the expected value of 1.25. Adding cetaceans to the analysis resulted in a small change of the fit (Fig. 3A, black line). Remarkably, the function fitted exclusively for lissencephalic species also predicted the relationship between $T^{1/2}A_G$ and $A_E$ in gyrencephalic species (Fig. 3A, green line)—and species such as the manatee and other afrotherians are no longer outliers.

Given the theoretical relation $T^{1/2}A_G = kA_E^{1.25}$, it follows that lissencephalic species (for which $A_G = A_E$) are those that meet the condition $T = k^2A_G^{1/2}$. In contrast, all species for which $T < k^2A_G^{1/2}$ are predicted to be gyrencephalic, with $A_G > A_E$ (the alternative where $T > k^2A_G^{1/2}$ would result in $A_G < A_E$, which is geometrically impossible). Indeed, in the combined data set, we find that $T \approx A_G^{0.555\pm0.053}$ ($P$ < 0.0001) across lissencephalic species (Fig. 3B, green line). All gyrencephalic species data points fall to the right of the lissencephalic distribution; that is, their $A_G$ values are larger than predicted for a cortical thickness that would allow lissencephaly. The precise relationship between $T$ and $A_G$ across gyrencephalic species differs across orders, with a much smaller exponent for primates than for artiodactyls (Fig. 3B, red and pink lines). Thus, within the single universal relationship that describes cortical expansion, there is a transition point between smooth and folded cortices: Gyrencephaly ensues when $A_G$ expands in area faster than $T^2$. For gyrencephalic species, the rate of expansion of cortical thickness relative to expansion of the cortical surface varies across orders, but the product $T^{1/2}A_G$ still varies as a universal function of $A_E^{1.26}$ to $A_E^{1.33}$.

We also found the same universality between the product $T^{1/2}A_G$ and $A_E$ across coronal sections

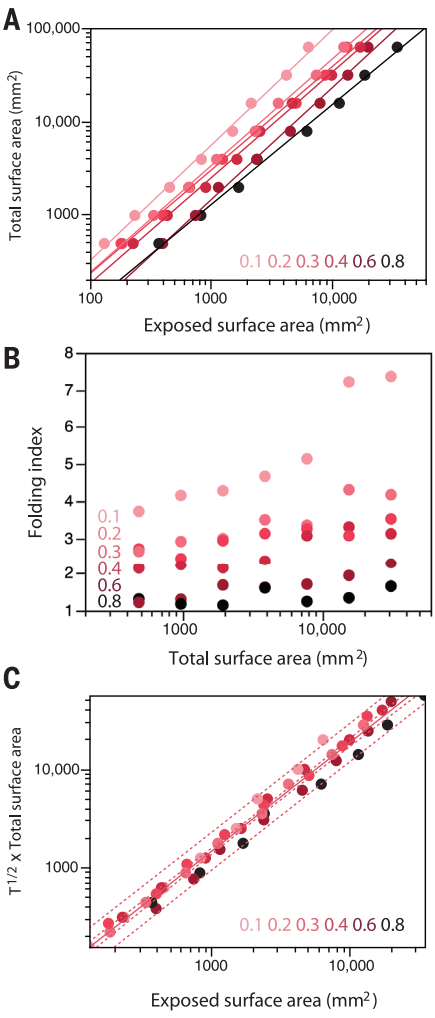


**Fig. 2. The degree of folding of crumpled paper balls is a function of surface area and thickness as predicted by our model.** (**A**) Relationship between total surface area of A4 to A11 sheets of office paper and the exposed surface area of the crumpled sheet of paper, with a power function of exponent 1.234 ± 0.033 for a single sheet of thickness 0.1 mm. (**B**) Increasing the thickness of the paper to be crumpled by stacking two to eight sheets displaces the curves to the right, that is, decreases the folding index of the resulting paper balls. (**C**) However, all crumpled paper balls of varying total surface area and thickness exhibit the same relationship, with the product $T^{1/2}A_T$ varying proportionately to $A_E^{1.105\pm0.022}$ ($r^2$ = 0.983, $P$ < 0.0001). Color gradations correspond to thickness in millimeters, as shown in each panel.

along the anteroposterior axis of the cortical hemisphere of a single individual, of different individuals, and even different species ranging from small rodents to human and elephant (fig. S1).

The finding that $A_E$ scales across all lissencephalic and gyrencephalic mammals (and even across species usually regarded as outliers such as the manatee and cetaceans) as a single power law of $T^{1/2}A_G$ indicates that gyrification is an intrinsic property of any mammalian cortex. Further, because the degree of folding can be described by the simple equation generated by our model (which also applies to crumpled sheets of paper), folding must occur as it minimizes the effective free energy of the cortical surface. Folding is therefore an intrinsic, fractal property of a self-avoiding surface, whether biological or not, subjected to crumpling forces. As such, this scaling of cortical folding does not depend on numbers of neurons or how they are distributed in the cortical sheet, but simply on the relative lateral expansion of this sheet relative to its thickness, regardless of how densely neurons are distributed within it.

The finding that cortical folding scales universally across clades, species, individuals, and parts of the same cortex implies that the single mechanism based on the physics of minimization of effective free energy of a growing surface subject to inhomogeneous bulk stresses applies across cortical development and evolution. This is in stark contrast to previous conclusions that different mechanisms regulated folding at different levels (*7*); such conclusions may reflect the traditional emphasis on the relationship between folding degree and brain volume (*1*, *8*), which is indeed diverse across orders, across species, and across individuals of a same species (*6*, *8*). Also, the dependence of cortical folding on a simple combination of $A_G$ and $T$ implies that any alterations, such as defects in cell migration, that lead to increased $T$ or decreased $A_G$ (or both) are expected to decrease cortical folding, exactly as found in human pathological lissencephaly (*28*). This might also be the case for the lissencephalic brain of birds, where a very thick telencephalon of small surface area surrounds the subpallial structures.

Finally, our findings indicate that cortical folding did not evolve, in the sense of a new property specific to some clades but not others. Similarly, there is no such thing as "secondary lissencephaly" (*29*), nor are there two clusters of gyrencephaly (*9*). Rather, what has evolved, we propose, is a faster increase in $A_G$ relative to $T^2$ in development—and at different rates in different mammalian clades, which thus become gyrencephalic at different functions of $A_G$ or different numbers of neurons.

Remarkably, there is no a priori reason for lissencephaly, considering that $A_G$ and $T$ ultimately result from different biological processes: lateral expansion of the progenitor cell population for $A_G$, radial neurogenesis and cell growth for $T$ (*30*). Similarly, there is no a priori reason for the cortex to become gyrencephalic once past a certain surface area—unless the rate of (lateral) progenitor cell expansion inevitably outpaces the rate of (radial) neurogenesis at this point, which apparently occurs typically when $A_G$ reaches 400 mm$^2$. We propose that, starting from the earliest and smallest (and smooth) mammalian brains (*31*), the cortical surface initially scaled isometrically, with $A_G \approx T^2$. Gyrencephaly ensued in each clade as soon as this lockstep growth changed, with $A_G$ now increasing faster than $T^2$. Probable mechanisms involved are those that control the rate of neurogenesis and increases in cell size relative to the rate of progenitor and intermediate progenitor cell proliferation in early cortical development. Rapid increases in numbers of intermediate progenitor cells would lead to gyrencephaly, although not through the generation of larger numbers of neurons, as previously thought (*7*, *30*, *32*), but rather through the simple lateral expansion of the resulting cortical surface area at a rate faster than the cortical thickness squared.

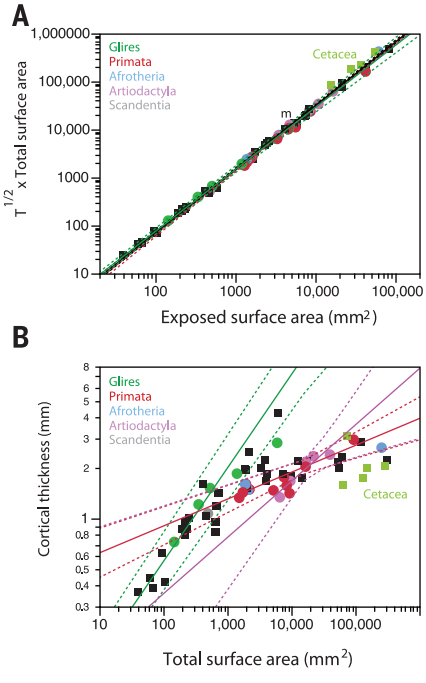


**Fig. 3. The degree of folding of the mammalian cerebral cortex is a single function of surface area and thickness across lissencephalic and gyrencephalic species alike, although thickness scales as order-specific functions of cortical surface area.** (**A**) The product $T^{1/2}A_G$ varies with $A_E^{1.329\pm0.014}$ ($r^2$ = 0.996, $P < 0.0001$) across noncetacean gyrencephalic species in the combined data set (red line), with $A_E^{1.325\pm0.009}$ ($r^2$ = 0.997, $P < 0.0001$, $k = 0.157 \pm 0.012$) across all species (including cetaceans; black line), and with $A_E^{1.292\pm0.027}$ ($r^2$ = 0.994, $P < 0.0001$) across lissencephalic species alone (green line). Note that the function plotted for lissencephalic species predicts the product $T^{1/2}A_G$ for gyrencephalic species equally well as the functions plotted for gyrencephalic species themselves. (**B**) Cortical thickness varies with cortical surface area $A_G^{0.555\pm0.053}$ ($r^2 = 0.887$, $P < 0.0001$) across lissencephalic species in the combined data set (green line), but with $A_G^{0.160\pm0.025}$ ($r^2 = 0.703$, $P < 0.0001$) across primates (red line), and with $A_G^{0.334\pm0.072}$ ($r^2$ = 0.879, $P$ = 0.0185) across artiodactyl species (pink line). All fits exclude cetaceans. Dashed lines indicate the 95% confidence intervals for the fitted functions.

## REFERENCES AND NOTES


1. M. A. Hofman, *Brain Behav. Evol.* **27**, 28–40 (1985).
2. A. J. Rockel, R. W. Hiorns, T. P. Powell, *Brain* **103**, 221–244 (1980).
3. P. Rakic, *Trends Neurosci.* **18**, 383–388 (1995).
4. R. Toro, Y. Burnod, *Cereb. Cortex* **15**, 1900–1913 (2005).
5. T. Tallinen, J. Y. Chung, J. S. Biggins, L. Mahadevan, *Proc. Natl. Acad. Sci. U.S.A.* **111**, 12667–12672 (2014).
6. K. Zilles, N. Palomero-Gallagher, K. Amunts, *Trends Neurosci.* **36**, 275–284 (2013).
7. E. Lewitus, I. Kelava, W. B. Huttner, *Front. Hum. Neurosci.* **7**, 424 (2013).
8. P. Pillay, P. R. Manger, *Eur. J. Neurosci.* **25**, 2705–2712 (2007).
9. E. Lewitus, I. Kelava, A. T. Kalinka, P. Tomancak, W. B. Huttner, *PLOS Biol.* **12**, e1002000 (2014).
10. F. A. C. Azevedo *et al.*, *J. Comp. Neurol.* **513**, 532–541 (2009).
11. M. Gabi *et al.*, *Brain Behav. Evol.* **76**, 32–44 (2010).
12. S. Herculano-Houzel, B. Mota, R. Lent, *Proc. Natl. Acad. Sci. U.S.A.* **103**, 12138–12143 (2006).
13. S. Herculano-Houzel, C. E. Collins, P. Wong, J. H. Kaas, *Proc. Natl. Acad. Sci. U.S.A.* **104**, 3562–3567 (2007).
14. S. Herculano-Houzel *et al.*, *Brain Behav. Evol.* **78**, 302–314 (2011).
15. S. Herculano-Houzel *et al.*, *Front. Neuroanat.* **8**, 46 (2014).
16. R. S. Kazu, J. Maldonado, B. Mota, P. R. Manger, S. Herculano-Houzel, *Front. Neuroanat.* **8**, 128 (2014).
17. K. Neves *et al.*, *Front. Neuroanat.* **8**, 5 (2014).
18. D. K. Sarko, K. C. Catania, D. B. Leitch, J. H. Kaas, S. Herculano-Houzel, *Front. Neuroanat.* **3**, 8 (2009).
19. S. Herculano-Houzel, B. Mota, P. Wong, J. H. Kaas, *Proc. Natl. Acad. Sci. U.S.A.* **107**, 19008–19013 (2010).
20. L. Ventura-Antunes, B. Mota, S. Herculano-Houzel, *Front. Neuroanat.* **7**, 3 (2013).
21. P. F. M. Ribeiro *et al.*, *Front. Neuroanat.* **7**, 28 (2013).
22. H. Elias, D. Schwartz, *Z. Saugetierkd.* **36**, 147–163 (1971).
23. R. L. Reep, T. J. O'Shea, *Brain Behav. Evol.* **35**, 185–194 (1990).
24. T. M. Mayhew, G. L. Mwamengele, V. Dantzer, S. Williams, *J. Anat.* **188**, 53–58 (1996).
25. Y. Kantor, M. Kardar, D. R. Nelson, *Phys. Rev. A* **35**, 3056–3071 (1987).
26. D. H. Smith, *Prog. Neurobiol.* **89**, 231–239 (2009).
27. D. H. Smith, J. A. Wolf, D. F. Meaney, *Tissue Eng.* **7**, 131–139 (2001).
28. S. E. Hong *et al.*, *Nat. Genet.* **26**, 93–96 (2000).
29. I. Kelava, E. Lewitus, W. B. Huttner, *Front. Neuroanat.* **7**, 16 (2013).
30. J. H. Lui, D. V. Hansen, A. R. Kriegstein, *Cell* **146**, 18–36 (2011).
31. T. B. Rowe, T. E. Macrini, Z. X. Luo, *Science* **332**, 955–957 (2011).
32. I. Reillo, C. de Juan Romero, M. A. García-Cabezas, V. Borrell, *Cereb. Cortex* **21**, 1674–1694 (2011).


## ACKNOWLEDGMENTS

Supported by Conselho Nacional de Desenvolvimento Científico e Tecnológico, Fundação de Amparo à Pesquisa do Estado do Rio de Janeiro, INCT/MCT, and the James S. McDonnell Foundation. Data reported in the paper are presented in the supplementary materials.

## SUPPLEMENTARY MATERIALS

www.sciencemag.org/content/349/6243/74/suppl/DC1
Materials and Methods
Table S1
References (*33*–*38*)

13 February 2015; accepted 11 May 2015
10.1126/science.aaa9101

Science
AAAS

# Cortical folding scales universally with surface area and thickness, not number of neurons

Bruno Mota and Suzana Herculano-Houzel

*Science* **349**, 74 (2015);
DOI: 10.1126/science.aaa9101

*This copy is for your personal, non-commercial use only.*

**If you wish to distribute this article to others**, you can order high-quality copies for your colleagues, clients, or customers by clicking here.

**Permission to republish or repurpose articles or portions of articles** can be obtained by following the guidelines here.

***The following resources related to this article are available online at www.sciencemag.org (this information is current as of July 2, 2015 ):***

**Updated information and services,** including high-resolution figures, can be found in the online version of this article at:
http://www.sciencemag.org/content/349/6243/74.full.html

**Supporting Online Material** can be found at:
http://www.sciencemag.org/content/suppl/2015/07/01/349.6243.74.DC1.html

A list of selected additional articles on the Science Web sites **related to this article** can be found at:
http://www.sciencemag.org/content/349/6243/74.full.html#related

This article **cites 37 articles**, 10 of which can be accessed free:
http://www.sciencemag.org/content/349/6243/74.full.html#ref-list-1

This article has been **cited by** 1 articles hosted by HighWire Press; see:
http://www.sciencemag.org/content/349/6243/74.full.html#related-urls

This article appears in the following **subject collections:**
Neuroscience
http://www.sciencemag.org/cgi/collection/neuroscience

Downloaded from www.sciencemag.org on July 2, 2015

*Science* (print ISSN 0036-8075; online ISSN 1095-9203) is published weekly, except the last week in December, by the American Association for the Advancement of Science, 1200 New York Avenue NW, Washington, DC 20005. Copyright 2015 by the American Association for the Advancement of Science; all rights reserved. The title *Science* is a registered trademark of AAAS.